Unsymmetrical A-Frame Pt_2Pd Trinuclear Complexes: Site-Selective Apparent Double Insertion of Alkynes into Pd−Pt and Pd−P Bonds

Tomoaki Tanase* and Rowshan Ara Begum

Department of Chemistry, Faculty of Science, Nara Women's University, Kitauoya-higashi-machi, Nara 630-8285, Japan

Received August 28, 2000

Reactions of the linearly ordered Pt_2Pd mixed-metal complex *linear*-$[Pt_2Pd(\mu\text{-dpmp})_2(XylNC)_2](PF_6)_2$ (**1b**) (dpmp = bis(diphenylphosphinomethyl)phenylphosphine, XylNC = 2,6-xylyl isocyanide), with electron-deficient alkynes, RC≡CR′, led to the formation of a series of unsymmetrical A-frame clusters formulated as $[Pt_2Pd(\mu\text{-dpmp})(\mu\text{-}Ph_2PCH_2P(Ph)CH_2P(Ph)_2\text{-}CRCR')(XylNC)_2](PF_6)_2$ (R = R′ = CO_2Me (**2**); R = R′ = CO_2Et (**3**); R = H, R′ = CO_2Me (**4**); R = H, R′ = CO_2Et (**5**); R = CH_3, R′ = CO_2Et (**6**)) in considerable yields, in which the alkyne molecule was site-selectively inserted into the Pt−Pd bond and was further reacted with a phosphine unit of a dpmp ligand through double bond breaking of the C≡C unit. Complexes **2**−**6** were characterized by IR, electronic absorption, and NMR spectroscopic techniques and X-ray crystallography (**2**, **4**, and **5**) to reveal that the apparent double insertion of the acetylene unit takes place site-selectively on the Pt−Pd−P heterometallic center. In complexes **4** and **5**, the P−C bond formation occurred regioselectively between the terminal alkyne carbon and phosphine unit of dpmp, resulting in a $\mu\text{-}\eta^1\text{:}\eta^2$-phosphorus C_2 ylide bridging structure. The reaction mechanism was discussed. In contrast, reaction of **1b** with excess HBF_4 afforded $[Pt_2Pd(\mu\text{-H})(dpmp)_2(XylNC)_2](BF_4)_3$ (**8**), where a proton was oxidatively added to the Pt−Pt bond vs the Pt−Pd bond. From the X-ray crystal structure of **8**, the structural change accompanied by the addition was revealed to be fairly small, with a slight elongation of the Pt−Pt bond from 2.690(1) Å (**1b**) to 2.867(2) Å (**8**). These results demonstrated that the heterometal (Pd) was able to alter the reactivity of the linear trimetallic clusters and interestingly regulated its specificity.

Introduction

Metal−metal bonded small clusters of platinum and palladium have been of potential interest as minimal models for the surface of heterogeneous catalysts and as new homogeneous catalysts and fine-tunable photo- and electrochemical materials.[1] We have studied the synthesis and characterization of homo- and heterometallic di- and trinuclear Pt and Pd complexes supported by a tridentate phosphine ligand, bis(diphenylphosphinomethyl)phenylphosphine (dpmp).[2] During our studies, the linearly ordered triplatinum cluster *linear*-$[Pt_3(\mu\text{-dpmp})_2(XylNC)_2](PF_6)_2$ (**1a**)[2d] has been prepared by site-selective incorporation of Pt^0 atom into the dpmp-bridged diplatinum complex $[Pt_2(\mu\text{-dpmp})_2(XylNC)_2](PF_6)_2$. Compound **1a** possesses a widespread, coordinatively unsaturated plane comprised of the three platinum atoms with 44 valence electrons and is, thus, of general interest as a simple model for the interactions of metal surfaces with small organic molecules. Some reactions of **1a** with small molecules and ions, activated alkynes, electron-deficient isocyanide, H^+, and NO^+, have already been examined to afford a series of unsymmetrical A-frame triplatinum complexes,[2j] $[Pt_3(\mu\text{-dpmp})_2(\mu\text{-RC═CR′})(XylNC)_2]^{2+}$ (R = R′ = CO_2Me, CO_2Et; R = H, R′ = CO_2Me), $[Pt_3(\mu\text{-dpmp})_2(RNC)(XylNC)_2]^{2+}$ (R = *p*-$NO_2C_6H_4$), and $[Pt_3(\mu\text{-H})(\mu\text{-dpmp})_2(XylNC)_2]^{3+}$, and a double A-frame cluster,[2c] $[Pt_3(\mu\text{-NO})_2(\mu\text{-dpmp})_2(XylNC)_2]^{4+}$. The analogous Pt_2Pd heterotrimetallic cluster, *linear*-$[Pt_2Pd(\mu\text{-dpmp})_2(XylNC)_2](PF_6)_2$ (**1b**), has also been prepared by reaction of the Pd^0 atom with $[Pt_2(\mu\text{-dpmp})_2(XylNC)_2](PF_6)_2$ and characterized by X-ray crystallography to involve a linearly ordered Pt−Pt−Pd core.[2d] Detailed studies on mixed-metal clusters could provide useful information concerning the development of industrial heterogeneous catalysts containing two or more different metals and could

* To whom correspondence should be addressed. Fax: +81 742−20−3399. E-mail: tanase@cc.nara-wu.ac.jp.

(1) (a) Adams, D. A., Cotton, F. A., Eds. *Ctalysis by Di- and Polynuclear Metal Cluster Complexes*; Wiley-VCH: New York, 1998. (b) Balch, A. L. In *Progress in Inorganic Chemistry*; Lippard, S. J., Ed.; Wiley: New York, 1994; Vol. 41, p 239. (c) Balch, A. P. In *Homogeneous Catalysis with Metal Phosphine Complexes*; Pignolet, L. H., Ed.; Plenum Press: New York, 1983; p 167.

(2) (a) Tanase, T.; Yamamoto, Y. *Trends Organomet. Chem*. **1999**, *3*, 31. (b) Tanase, T.; Masuda, K.; Hamaguchi, M.; Begum, R. A.; Yano, S. *Inorg. Chem. Acta* **2000**, *299*, 99. (c) Tanase, T.; Hamaguchi, M.; Begum, R. A.; Yano, S.; Yamamoto, Y. *Chem. Commun*. **1999**, 745. (d) Tanase, T.; Ukaji, H.; Takahata, H.; Toda, T.; Yamamoto, Y. *Organometallics* **1998**, *17*, 196. (e) Tanase, T.; Toda, T.; Yamamoto, Y. *Inorg. Chem*. **1997**, *36*, 1571. (f) Tanase, T.; Takahata, H.; Ukaji, H.; Hasegawa, M.; Yamamoto, Y. *J. Organomet. Chem*. **1997**, *538*, 247. (g) Tanase, T.; Igoshi, T.; Yamamoto, Y. *Inorg. Chim. Acta* **1997**, *256*, 61. (h) Tanase, T.; Takahata, H.; Yamamoto, Y. *Inorg. Chim. Acta* **1997**, *264*, 5. (i) Tanase, T.; Takahata, H.; Hasegawa, M.; Yamamoto, Y. *J. Organomet. Chem*. **1997**, *545/546*, 531. (j) Tanase, T.; Ukaji, H.; Igoshi, T.; Yamamoto, Y. *Inorg. Chem*. **1996**, *35*, 4114. (k) Tanase, T.; Toda, H.; Kobayashi, K.; Yamamoto, Y. *Organometallics* **1996**, *15*, 5272.

10.1021/om000747y CCC: $20.00
Publication on Web 12/08/2000

also lead to the development of new homogeneous catalytic reactions that are not established by mononuclear centers.[3] In the present study, we have examined the reactivity of a mixed-metal Pt_2Pd cluster (**1b**), in particular, with electron-deficient alkynes and have found that a novel, apparent double insertion of the acetylene unit into the Pt−Pd and Pd−P bonds occurred site-selectively on the Pt−Pd heterometallic site. We wish to report herein the synthesis and characterizations of the unsymmetrical heterotrimetallic A-frame clusters $[Pt_2Pd(\mu\text{-dpmp})(\mu\text{-}Ph_2PCH_2P(Ph)CH_2P(Ph)_2\text{-}CRCR')(XylNC)_2](PF_6)_2$ (R = R′ = CO_2Me (**2**); R = R′ = CO_2Et (**3**); R = H, R′ = CO_2Me (**4**); R = H, R′ = CO_2Et (**5**); R = CH_3, R′ = CO_2Et (**6**)). It should be noted that the similar double insertion of the electron-deficient alkynes was not promoted by the homometallic analogous clusters *linear*-$[M_3(\mu\text{-dpmp})_2(XylNC)_2](PF_6)_2$ (M = Pt (**1a**), M= Pd (**1c**)). In addition, we wish to report a proton adduct of **1b**, $[Pt(\mu\text{-H})PtPd(\mu\text{-dpmp})_2(XylNC)_4](BF_4)_3$ (**8**), where H^+ ion was oxidatively added between the Pt−Pt bond to form the hydride-bridged unsymmetrical trimetallic A-frame cluster.

Experimental Section

Solvents were dried and freshly distilled prior to use. Other reagents were of the best commercial grade and were used as received. *linear*-$[Pt_2Pd(dpmp)_2(XylNC)_2](PF_6)_2\cdot(CH_3)_2CO$ (**1b**) was prepared by the methods already reported.[2d] All reactions were carried out under a nitrogen atmosphere with standard Schlenk and vacuum line techniques.

Measurement. ^1H NMR spectra were measured on a Bruker AC 250 (at 250 MHz) and Varian Gemini 2000 (at 300 MHz) instruments. Chemical shifts were calibrated to tetramethylsilane as an external reference. $^{31}P\{^1H\}$ NMR spectra were recorded by the same instruments at 121 or 101 MHz, chemical shifts being calibrated to 85% H_3PO_4 as an external reference. Infrared and electronic absorption spectra were recorded with Shimadzu UV3000 and Jasco FT/IR-410 spectrometers, respectively.

Preparation of $[Pt_2Pd(\mu\text{-dpmp})(\mu\text{-}Ph_2PCH_2P(Ph)CH_2P(Ph)_2CRCR')(XylNC)_2](PF_6)_2$ (2: R = R′ = CO_2Me; 3: R = R′ = CO_2Et; 4: R = H, R′ = CO_2Me; 5: R = H, R′ = CO_2Et; 6: R = Me, R′ = CO_2Et). Complex 2. To a dichloromethane solution (30 mL) containing *linear*-$[Pt_2Pd(dpmp)_2(XylNC)_2](PF_6)_2\cdot(CH_3)_2CO$ (**1b**) (72 mg, 0.034 mmol) was added acetylenedicarboxylic acid dimethyl ester (65 mg, 0.46 mmol). The solution was stirred at room temperature for 3 h. The solvent was removed under reduced pressure, and the residue was washed with diethyl ether, followed by recrystallization from dichloromethane/diethyl ether mixed solvent, to give pale orange crystals of $[Pt_2Pd(\mu\text{-dpmp})(\mu\text{-}Ph_2PCH_2P(Ph)CH_2P(Ph)_2C(CO_2Me)C(CO_2Me))(XylNC)_2](PF_6)_2$ (**2**), which were separated by filtration, washed with diethyl ether, and dried in vacuo (62 mg, yield 83%). Anal. Calcd for $C_{88}H_{82}N_2O_4P_8F_{12}Pt_2Pd$: C, 47.96; H, 3.75; N, 1.27. Found: C, 47.81; H, 3.66; N, 1.17. IR (Nujol): ν(N≡C) 2169, 2129, ν(C═O) 1700, 1685, $\nu(PF_6)$ 838 cm^{-1}. UV−vis (in CH_2Cl_2): λ_{max} (log ϵ) 351 (4.947) nm. ^1H NMR (in acetone-d_6): δ 1.48 (s, *o*-Me, 6H), 1.80 (s, *o*-Me, 6H), 2.30 (s, OMe, 3H), 3.19 (s, OMe, 3H), 3.6−5.8 (m, CH_2, 8H), 6.9−8.2 (m, Ar, 56H). $^{31}P\{^1H\}$ NMR (in acetone-d_6): δ 29.0 (br s, 1P, $^3J_{PtP}$ = 159 Hz), 25.2 (br d, 1P, $J_{PP'}$ = 104 Hz), 9.3 (br m, 2P, $^1J_{PtP}$ not resolved), 0.3 (m, 1P, $^1J_{PtP}$ = 2943 Hz), −2.3 (m, 1P, $^1J_{PtP}$ = 2765 Hz).

Complex 3. To a dichloromethane solution (30 mL) containing **1b** (74 mg, 0.035 mmol) was added acetylenedicarboxylic acid diethyl ester (64 mg, 0.38 mmol). The solution was stirred at room temperature for 3 h. The solvent was removed under reduced pressure, and the residue was washed with diethyl ether, followed by recrystallization from dichloromethane/diethyl ether mixed solvent, to give pale orange crystals of $[Pt_2Pd(\mu\text{-dpmp})(\mu\text{-}Ph_2PCH_2P(Ph)CH_2P(Ph)_2C(CO_2Et)C(CO_2Et))(XylNC)_2](PF_6)_2\cdot0.5CH_2Cl_2$ (**3**·$0.5CH_2Cl_2$) (41 mg, yield 52%). Anal. Calcd for $C_{90.5}H_{87}N_2O_4P_8F_{12}ClPt_2Pd$: C, 47.79; H, 3.86; N, 1.23. Found: C, 47.91; H, 3.72; N, 1.16. IR (Nujol): ν(N≡C) 2159, 2128, ν(C═O) 1708, 1685, $\nu(PF_6)$ 836 cm^{-1}. UV−vis (in CH_2Cl_2): λ_{max} (log ϵ) 346 (4.985) nm. ^1H NMR (in CD_2Cl_2): δ 1.35 (s, *o*-Me, 6H), 1.71 (s, *o*-Me, 6H), 0.27 (t, OCH_2CH_3, 3H), 0.73 (t, OCH_2CH_3, 3H), 2.64, 2.90 (d × q (AB), OCH_2CH_3, 2H, $J_{HH'}$ = 11 Hz), 3.45, 3.83 (d × q (AB), OCH_2CH_3, 2H, $J_{HH'}$ = 11 Hz), 3.0−5.2 (m, CH_2, 8H), 6.4−8.1 (m, Ar, 56H). $^{31}P\{^1H\}$ NMR (in acetone-d_6): δ 28.3 (br s, 1P, $^3J_{PtP}$ = 159 Hz), 25.0 (br d, 1P, $J_{PP'}$ = 99 Hz), broad signals were observed around 15 to −20 ppm (4P).

Complex 4. Pale orange crystals of $[Pt_2Pd(\mu\text{-dpmp})(\mu\text{-}Ph_2PCH_2P(Ph)CH_2P(Ph)_2CHC(CO_2Me))(XylNC)_2](PF_6)_2$ (**4**) were obtained in 74% yield (50 mg) by a procedure similar to that described above from the reaction of **1b** (67 mg, 0.032 mmol) with HC≡CCO_2Me (65 mg, 0.77 mmol) for 3 h. Anal. Calcd for $C_{86}H_{80}N_2O_2P_8F_{12}Pt_2Pd$: C, 48.13; H, 3.76; N, 1.31. Found: C, 48.15; H, 3.75; N, 1.27. IR (Nujol): ν(N≡C) 2126, ν(C═O) 1645, $\nu(PF_6)$ 836 cm^{-1}. UV−vis (in CH_2Cl_2): λ_{max} (log ϵ) 348 (4.952), 428^{sh} (3.955) nm. ^1H NMR (in acetone-d_6): δ 1.49 (s, *o*-Me, 6H), 1.89 (s, *o*-Me, 6H), 3.50 (s, OMe, 3H), 4.12 (d x d, CH, 1H, $^2J_{PH}$ = 22 Hz, $^4J_{PH}$ = 6 Hz), 3.1−5.3 (m, CH_2, 8H), 6.5−8.6 (m, Ar, 56H). $^{31}P\{^1H\}$ NMR (in acetone-d_6): δ 29.0 (m, 1P, $^3J_{PtP}$ = 216 Hz), 15.8 (d × m, 1P, $J_{PP'}$ = 95 Hz), 9.5 (d × m, 1P, $^1J_{PtP}$ = 3155 Hz, $^2J_{PP'}$ = 501 Hz), 1.2 (d × m, 1P, $^1J_{PtP}$ not resolved, $^2J_{PP'}$ = 368 Hz), −4.9 (d × m, 1P, $^1J_{PtP}$ = 2585 Hz, $^2J_{PP'}$ = 368 Hz), −12.4 (d × m, 1P, $^1J_{PtP}$ = 2940 Hz, $^2J_{PP'}$ = 501 Hz).

Complex 5. Pale orange crystals of $[Pt_2Pd(\mu\text{-dpmp})(\mu\text{-}Ph_2PCH_2P(Ph)CH_2P(Ph)_2CHC(CO_2Et))(XylNC)_2](PF_6)_2$ (**5**) were obtained in 56% yield (47 mg) by the reaction of **1b** (82 mg, 0.039 mmol) with HC≡CCO_2Et (76 mg, 0.78 mmol) for 3 h. Anal. Calcd for $C_{87}H_{82}N_2O_2P_8F_{12}Pt_2Pd$: C, 48.38; H, 3.83; N, 1.30. Found: C, 48.25; H, 3.65; N, 1.20. IR (Nujol): ν(N≡C) 2127, ν(C═O) 1662, $\nu(PF_6)$ 838 cm^{-1}. UV−vis (in CH_2Cl_2): λ_{max} (log ϵ) 348 (4.879), 432^{sh} (3.851) nm. ^1H NMR (in acetone-d_6): δ 1.49 (s, *o*-Me, 6H), 1.91 (s, *o*-Me, 6H), 0.92 (t, OCH_2CH_3, 3H), 3.98 (q, OCH_2CH_3, 2H), 4.08 (d × d, CH, 1H, $^2J_{PH}$ = 22 Hz, $^4J_{PH}$ = 8 Hz), 3.1−5.3 (m, CH_2, 8H), 6.5−8.6 (m, Ar, 56H). $^{31}P\{^1H\}$ NMR (in acetone-d_6): δ 28.8 (m, 1P, $^3J_{PtP}$ = 217 Hz), 15.6 (d × m, 1P, $J_{PP'}$ = 99 Hz,), 9.9 (d × m, 1P, $^1J_{PtP}$ = 3160 Hz, $^2J_{PP'}$ = 501 Hz), 1.1 (d × m, 1P, $^1J_{PtP}$ not resolved, $^2J_{PP'}$ = 400 Hz), −4.8 (d × m, 1P, $^1J_{PtP}$ = 2208 Hz, $^2J_{PP'}$ = 400 Hz), −12.2 (d × m, 1P, $^1J_{PtP}$ = 2895 Hz, $^2J_{PP'}$ = 501 Hz).

Complex 6. Pale orange crystals of $[Pt_2Pd(\mu\text{-dpmp})(\mu\text{-}Ph_2PCH_2P(Ph)CH_2P(Ph)_2C(CH_3)C(CO_2Et))(XylNC)_2](PF_6)_2$ (**6**) were obtained in 58% yield (37 mg) by the reaction of **1b** (62 mg, 0.029 mmol) with CH_3C≡CCO_2Et (183 mg, 1.63 mmol) for 4 days at room temperature. Anal. Calcd for $C_{88}H_{84}N_2O_2P_8F_{12}Pt_2Pd$: C, 48.62; H, 3.89; N, 1.29. Found: C, 48.38; H, 3.84; N, 1.21. IR (Nujol): ν(N≡C) 2147, 2114, ν(C═O) 1640, $\nu(PF_6)$ 834 cm^{-1}. UV−vis (in CH_2Cl_2): λ_{max} (log ϵ) 351 (4.981), 441^{sh} (3.967) nm. ^1H NMR (in CD_2Cl_2): δ 0.80 (br, OCH_2CH_3, 3H), 1.31 (s, *o*-Me, 6H), 1.90 (s, *o*-Me, 6H), 2.11 (CCH_3, 3H), 2.75 (br, $CO_2CH_2CH_3$, 2H), 3.2−5.4 (m, CH_2, 8H), 6.5−8.2 (m, Ar, 56H). $^{31}P\{^1H\}$ NMR (in acetone-d_6): δ 33.3 (br, 1P, $^3J_{PtP}$ = 216 Hz), 15.8 (br d, 1P, $J_{PP'}$ = 95 Hz), broad signals were observed around 15 to −20 ppm (4P).

Preparation of $[Pt_2Pd(\mu\text{-H})(\mu\text{-dpmp})_2(XylNC)_2](BF_4)_3\cdot CH_2Cl_2$ (8·CH_2Cl_2). To a CH_2Cl_2 solution (10 mL) containing **1b** (50 mg, 0.024 mmol) was added $HBF_4\cdot(CH_3)_2O$ (142 mg, 1.06 mmol). The solution was stirred at room temperature for 30 min. The color of the solution immediately changed from orange to yellow. The solvent was removed under reduced

(3) Sinfelt, J. H. *Bimetallic Catalysis: Discoveries, Concepts and Applications*; Wiley: New York, 1983.

Table 1. Crystallographic and Experimental Data for 2·2CH_2Cl_2, 4·4.5CH_2Cl_2, 5·4CH_2Cl_2, and 8·3.5CH_2Cl_2·4H_2O

	2·2CH_2Cl_2	**4**·4.5CH_2Cl_2	**5**·4CH_2Cl_2	**8**·3.5CH_2Cl_2·4H_2O
formula	$C_{90}H_{86}N_2O_4P_8F_{12}Cl_4Pt_2Pd$	$C_{90.5}H_{89}N_2O_2P_8F_{12}Cl_9Pt_2Pd$	$C_{91}H_{90}N_2O_2P_8F_{12}Cl_8Pt_2Pd$	$C_{85.5}H_{92}N_2O_4P_6F_{12}B_3Cl_7Pt_2Pd$
fw	2373.84	2528.14	2499.70	2402.68
cryst syst	triclinic	triclinic	monoclinic	triclinic
space group	$P\bar{1}$ (No. 2)	$P\bar{1}$ (No. 2)	$P2/a$ (No. 13)	$P\bar{1}$ (No. 2)
a/Å	18.949(4)	14.518(3)	27.465(9)	18.147(7)
b/Å	19.555(4)	30.086(8)	12.246(3)	19.881(7)
c/Å	14.328(3)	11.631(3)	31.06(1)	14.850(5)
α/deg	96.81(2)	92.55(2)		99.82(4)
β/deg	110.01(1)	96.55(4)	103.50(4)	101.03(4)
γ/deg	106.52(2)	90.44(4)		93.17(5)
V/Å^3	4643(2)	5041(2)	10158(5)	5159(3)
Z	2	2	4	2
T/°C	−118	−118	−118	−138
D_{calcd}/g cm^{-3}	1.698	1.665	1.634	1.546
μ/cm^{-1}	35.12	33.67	33.15	32.07
F(000)	2340	2490	4928	2370
scan method	$\omega-2\theta$	$\omega-2\theta$	$\omega-2\theta$	$\omega-2\theta$
scan speed/deg min^{-1}	16	16	16	16
2θ max/deg	47	46	45	49
h,k,l range	$+h, \pm k, \pm l$	$+h, \pm k, \pm l$	$+h, +k, \pm l$	$+h, \pm k, \pm l$
no. of data	13 626	13 188	13 903	16 083
no. of obsd data	11 036 ($I > 2\sigma(I)$)	9982 ($I > 2\sigma(I)$)	6949 ($I > 2\sigma(I)$)	7409 ($I > 3\sigma(I)$)
solution	direct methods SIR92	direct methods SIR92	direct methods SIR92	direct methods SAPI92
no. of params	1109	1151	681	647
data/param	9.95	8.67	10.20	11.45
R[a]	0.037	0.048	0.076	0.096
R_w [a]	0.043	0.057	0.086	0.110
GOF[b]	1.49	1.46	1.46	2.40

[a] $R = \sum||F_o| - |F_c||/\sum|F_o|$; $R_w = [\sum w(|F_o| - |F_c|)^2/\sum w|F_o|^2]^{1/2}$ ($w = 1/\sigma^2(F_o)$). [b] GOF = $[\sum w(|F_o| - |F_c|)^2/(N_o - N_p)]^{1/2}$ (N_o = no. data, N_p = no. variables).

pressure, and the residue was washed with Et_2O, followed by recrystallization from dichloromethane/diethyl ether mixed solvent, to give yellow crystals of [$Pt_2Pd(\mu$-H)(μ-dpmp)$_2$(XylNC)$_2$]-(BF_4)$_3$·CH_2Cl_2 (**8**·CH_2Cl_2), which were collected by removing the mother liquor via cannula, washed with diethyl ether, and dried in vacuo (31 mg, yield 62%). Analytical and spectral data for **8**·CH_2Cl_2: Anal. Calcd for $C_{83}H_{79}N_2P_6B_3F_{12}Cl_2Pt_2Pd$: C, 47.06; H, 3.76; N, 1.32. Found: C, 47.34; H, 3.89; N, 1.22. IR (Nujol): ν(N≡C) 2199, 2168, $\nu(BF_4)$ 1052 cm^{-1}. UV−vis (in CH_2Cl_2): λ_{max} (log ϵ) 328 (4.741), 387 (4.614), 435^{sh} (4.146) nm. ^{1}H NMR (in CD_2Cl_2): δ 1.49, 1.66 (s, *o*-Me), 4.2−5.6 (m, CH_2), 6.4−8.1 (m, Ar), −8.21 (br, μ-H, $^1J_{PtH}$ = 640, 573 Hz). ^{31}P{^{1}H} NMR (in CD_2Cl_2): δ 11.8 (m, 2P, $^1J_{PtP}$ = 2210 Hz), −5.9 (m, 2P), 7.5 (m, 1P, $^1J_{PtP}$ = 2618 Hz).

Crystal Data and Intensity Measurements for 2·2CH_2Cl_2, 4·4.5CH_2Cl_2, 5·4CH_2Cl_2, and 8·3.5CH_2Cl_2·4H_2O. All the crystals were extremely delicate when separated from their mother liquors, and the crystals used in data collection were mounted on a top of a glass fiber with Paraton N oil at low temperature. Crystal data and experimental conditions are summarized in Table 1. All data were collected on a Rigaku AFC7R diffractometer equipped with graphite-monochromated Mo Kα (λ = 0.71069 Å) radiation at low temperature. The cell constants were obtained from least-squares refinement of 20−25 reflections with 20° < 2θ < 30°. Three standard reflections were monitored every 150 reflections and showed no systematic decrease in intensity. Reflection data were corrected for Lorentz−polarization and absorption effects (ψ-scan method).

Structure Solution and Refinement. The structure of **2**·2CH_2Cl_2 was solved by direct methods with SIR92.[4] Most non-hydrogen atoms were located initially, and subsequent Fourier syntheses gave the positions of other non-hydrogen atoms. The coordinates of all hydrogen atoms were calculated at ideal positions with a C−H distance of 0.95 Å and were not refined. The structure was refined on F with the full-matrix least-squares techniques minimizing $\sum w(|F_o| - |F_c|)^2$. Final refinement was carried out with anisotropic thermal parameters for all non-hydrogen atoms and converged to R = 0.037 and R_w = 0.043. The structure of **4**·4.5CH_2Cl_2 was solved and refined by procedures similar to those described for **2**. Final full-matrix least-squares refinement was carried out with anisotropic thermal parameters for all non-hydrogen atoms except the carbon atoms of solvent molecules to converge at R = 0.048 and R_w = 0.057. The C atoms of CH_2Cl_2 were refined isotropically. The position of H(77) bound to C(7) was determined by difference Fourier synthesis, and the other H atoms were calculated at ideal positions with C−H = 0.95 Å. All hydrogen atoms were fixed in the refinement. The structure of **5**·4CH_2Cl_2 was solved and refined by procedures similar to those described for **2**. The coordinates of all hydrogen atoms were calculated at ideal positions with a C−H distance of 0.95 Å and were not refined. Final refinement was carried out with anisotropic thermal parameters for the Pt, Pd, Cl, P, and F atoms and with isotropic ones for other non-hydrogen atoms to converge at R = 0.076 and R_w = 0.086. The structure of **8**·3.5CH_2Cl_2·4H_2O was solved by direct methods with SAPI92.[5] Most non-hydrogen atoms were located initially, and subsequent Fourier syntheses gave the positions of other non-hydrogen atoms. The position of H(1) atom was determined by difference Fourier synthesis, and the coordinates of other hydrogen atoms were calculated at ideal positions with a C−H distance of 0.95 Å. All hydrogen atoms were fixed in the refinement. Final refinement was carried out with anisotropic thermal parameters for the Pt, Pd, Cl, P, and F atoms and with isotropic ones for other non-hydrogen atoms to converge at R = 0.096 and R_w = 0.110. The solvent molecules of crystallization were considerably disordered and were refined

(4) Burla, M. C.; Camalli, M.; Cascarano, G.; Giacovazzo, C.; Polidori, G.; Spagna, R.; Viterbo, D. *J. Appl. Crystallogr.* **1989**, *22*, 389.

(5) Fan, H.-F. R-SAPI, Rigaku Co., Tokyo, Japan, 1988.

Scheme 1

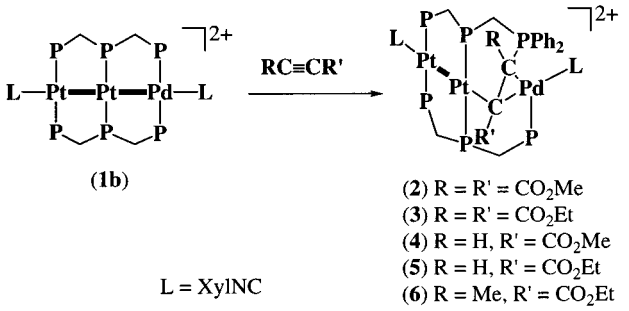

as $3.5CH_2Cl_2$ and $4H_2O$; these features led to a low-grade refinement of the present X-ray analysis for **8**.

Atomic scattering factors and values of f' and f'' for Pt, Pd, Cl, P, F, O, N, C, and B were taken from the literatures.[6] All calculations were carried out on a Silicon Graphics O2 Station with the teXsan Program System.[7] The perspective views were drawn by using the programs ORTEP-II.[8] Compilation of final atomic parameters for all non-hydrogen atoms is supplied as Supporting Information.

Results and Discussion

Reactions of *linear*-[$Pt_2Pd(\mu$-dpmp$)_2$(XylNC$)_2$]-($PF_6)_2$ (1b) with Electron-Deficient Alkynes. Reactions of **1b** with excess electron-deficient alkynes, RC≡CR′, in CH_2Cl_2 at room temperature afforded pale orange crystals formulated as [$Pt_2Pd(\mu$-dpmp$)(\mu$-$Ph_2PCH_2P(Ph)CH_2P(Ph)_2CRCR')$(XylNC$)_2$]($PF_6)_2$ (R = R′ = CO_2Me (**2**); R = R′ = CO_2Et (**3**); R = H, R′ = CO_2Me (**4**); R = H, R′ = CO_2Et (**5**); R = CH_3, R′ = CO_2Et (**6**)) in considerable yields (52−83%) (Scheme 1). The reaction with $CH_3C{\equiv}CCO_2Et$ proceeded slowly in comparison with those of the other alkynes and took 4 days to be completed. Nonactivated acetylenes, HC≡CPh and PhC≡CPh, were not reacted with **1b** under the same conditions. Complexes **2**−**6** are relatively stable in both solid and solution states. Elemental analysis indicated that complexes **2**−**6** are 1:1 adducts between the starting complex **1b** and the alkyne used. The electronic absorption spectra of **2**−**6** lost the characteristic peaks around 370−500 nm for the metal−metal bonded PtPtPd structure and showed only a band around 350 nm assignable to the $\sigma-\sigma^*$ transition of the Pt−Pt bond. These demonstrated that Pt−Pd bond breaking of the Pt_2Pd cluster core of **1b** took place during the reaction. The IR and ^{1}H NMR spectra of **2**−**6** indicated the presence of two unequivalent terminal isocyanide ligands. The IR spectra did not show the characteristic C═C stretching band around 1550 cm^{-1} as was observed in [$Pt_3(\mu$-dpmp$)_2(\mu$-RC═CR′)(XylNC$)_2$]($PF_6)_2$ (**7**) (Scheme 2).[2j] The $^{31}P\{^1H\}$ NMR spectra showed six unequivalent P atoms of dpmp ligands, suggesting an entirely unsymmetrical trinuclear structure. The $^{31}P\{^1H\}$ NMR spectrum of **4** consists of six resonances at δ 29.0 (A), 15.8 (A′), 9.5 (B), 1.2 (C), −4.9 (C′), and −12.4 (B′) (Figure 1). The resonances B, B′, C, and C′ were accompanied by ^{195}Pt satellite peaks ($^1J_{PtP}$ = 2585−3155 Hz) and showed

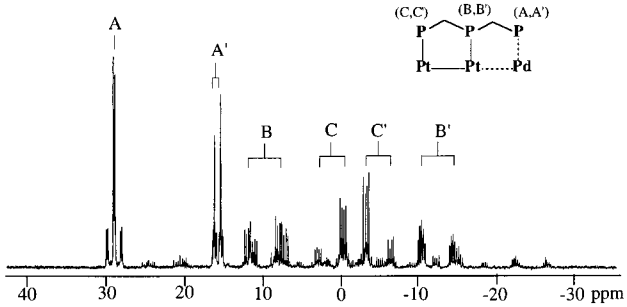

Figure 1. $^{31}P\{^1H\}$ NMR spectrum of [$Pt_2Pd(\mu$-dpmp$)(\mu$-$Ph_2PCH_2P(Ph)CH_2P(Ph)_2CHC(CO_2Me))$(XylNC$)_2$]($PF_6)_2$ (**4**) in acetone-d_6 at room temperature.

Scheme 2

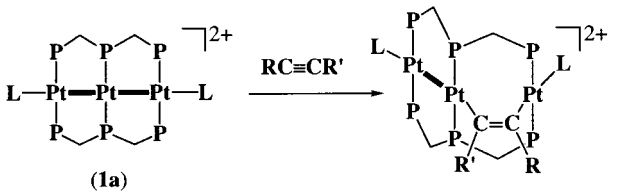

large *trans*-PP′ couplings ($^2J_{PP'}$ = 501 Hz (BB′) and 368 Hz (CC′)). The peaks A and A′ were not accompanied by Pt−P one-bond coupled ^{195}Pt satellites and did not strongly couple to each other. The resonance A (δ 29.0) is notably downfield-shifted from the chemical shift (δ 2.4) for the Pd-bound P nuclei in **1b**, which is in agreement with the presence of a phosphorus ylide moiety as described in the next section. In the ^{1}H NMR spectra of **4** and **5**, the resonances for the terminal alkyne proton appeared at about 4.1 ppm as a doublet of doublets with $^2J_{PH}$ = 22 Hz and $^4J_{PH}$ = 6−8 Hz, also implying a bond formation between a phosphine group of dpmp and the terminal alkyne carbon. These spectral features are consistent with the unsymmetrical Pt_2Pd structure determined by X-ray crystallography (vide infra).

Crystal Structures of [$Pt_2Pd(\mu$-dpmp$)(\mu$-Ph_2-$PCH_2P(Ph)CH_2P(Ph)_2CRCR')$(XylNC$)_2$]($PF_6)_2$ (R = R′ = CO_2Me (2); R = H, R′ = CO_2Me (4); R = H, R′ = CO_2Et (5)). The detailed structures of **2**, **4**, and **5** were determined by X-ray crystallography. The asymmetric unit of **2**·$2CH_2Cl_2$ contains a complex cation of **2**, two hexafluorophosphate anions, and two dichloromethane molecules. An ORTEP plot for the complex cation of **2** with the atomic numbering scheme is illustrated in Figure 2a, and selected bond lengths and angles are listed in Table 2. The complex cation of **2** consists of unsymmetrical Pt_2Pd trimetallic centers bridged by two dpmp ligands and terminally coordinated by two isocyanide ligands. The Pt(1)−Pt(2) bond length is 2.6792(4) Å and the Pt(2)···Pd(1) distance is 3.3453(7) Å, the former, slightly shorter than that of **1b** (2.690(1) Å), indicating the presence of a Pt−Pt single bond and the latter the absence of Pt−Pd bond. The alkyne molecule, $(C_2CO_2Me)_2$, was site-selectively inserted into the Pt−Pd σ-bond over the Pt−Pt bond and was further reacted with a phosphine unit of dpmp to form a novel μ-η^1:η^2 bridging structure of an acetylene C_2 unit (Figure 2b). In other words, the alkyne was doubly inserted into the Pt−Pd and the Pd−P bonds. Both the acetylene

(6) (a) Cromer, D. T.; Waber, J. T. *International Tables for X-ray Crystallography*; Kynoch Press: Birmingham, England, 1974; Vol. IV. (b) Cromer, D. T. *Acta Crystallogr.* **1965**, *18*, 17.

(7) *TEXSAN Structure Analysis Package*; Molecular Structure Corp.: The Woodlands, TX, 192.

(8) Johnson, C. K. *ORTEP-II*; Oak Ridge National Laboratory: Oak Ridge, TN, 1976.

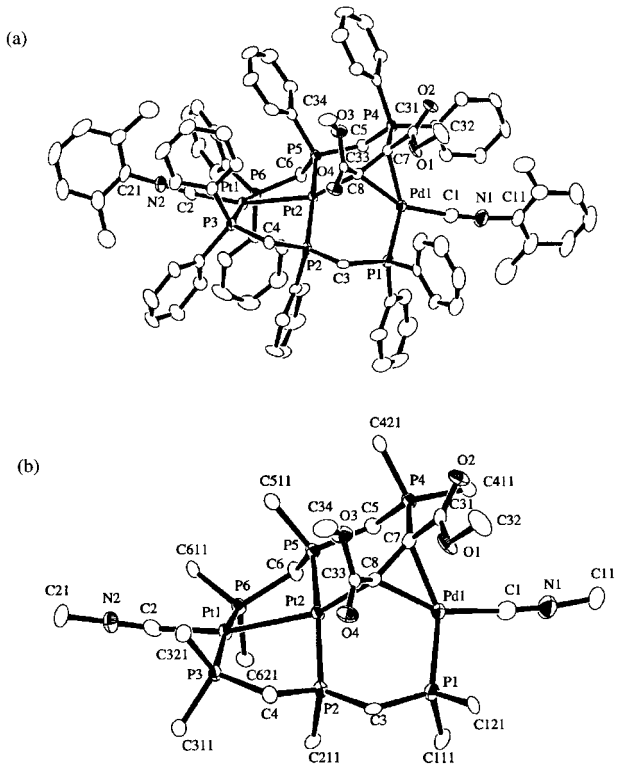

Figure 2. (a) ORTEP plot of the complex cation of **2**, $[Pt_2Pd(\mu\text{-dpmp})(\mu\text{-}Ph_2PCH_2P(Ph)CH_2P(Ph)_2C(CO_2Me)C(CO_2Me))(XylNC)_2]^{2+}$. (b) A close view of the cluster core of **2** with phenyl and xylyl rings omitted for clarity.

carbons (C(7), C(8)) adopt rather sp^3 tetrahedral configurations and the C(7)−C(8) bond length is 1.469(9) Å, which corresponds with a C−C single bond rather than to a C=C double bond.[9] The C(31)−C(7)−C(8)−C(32) torsion angle is 26.3(9)°. Consequently, the double bond breaking of the acetylene C_2 unit and the nucleophilic migration of the phosphine from Pd(1) to C(7) took place simultaneously during the reaction. The C(8) atom asymmetrically bridges the Pt(2) and Pd(1) atoms with Pt(2)−C(8) = 2.138(7) Å, Pd(1)−C(8) = 2.067(7) Å, and Pt(2)−C(8)−Pd(1) = 105.4(3)°. The Pd(1)−C(7) distance is 2.144(7) Å, which is appreciably longer than the Pd(1)−C(8) bond length. No interaction exists between the Pd(1) and P(4) atoms (Pd(1)···P(4) = 3.359(2) Å). The Pd(1) takes a distorted planar structure and is 0.15 Å out of the plane defined by C(1), C(7), C(8), and P(1) atoms. As to the acetylene and acetylide bridging systems,[10] many examples have been reported on $M_2(\mu\text{-}\eta^2\text{:}\eta^2\text{-RC≡CR}')$ (π,π)[11] and $M_2(\mu\text{-}\eta^1\text{:}\eta^2\text{-C≡CR}$ (σ,π)[12] structures (M = Pt and/or Pd), but the present asymmetrical bridging structure is not common. Recently, H. Kurosawa et al. reported the PtPd dinuclear complexes with the $\mu\text{-}\eta^2\text{:}\eta^3$ propargyl ligand, $[(PPh_2)Pt(\mu\text{-}\eta^2\text{:}\eta^3\text{-}t\text{BuCCCH}_2)Pd(C_6F_5)(PPh_3)]$,[13] in which the Pt−C interactions are 2.022(6)−2.063(6) Å via a η^2-mode and the Pd−C interactions are 2.142(6)−2.304(6) Å in η^3-fashion. Puddephatt et al. have reported reactions of the triangular Pt_3 and Pd_3 complexes, $[M_3(\mu_3\text{-CO})(\mu\text{-dppm})_3]^{2+}$ (M = Pt, Pd), with alkynes (dppm = bis(diphenylphosphino)methane); the alkynes, including acetylene, were oxidatively added to the coordinatively unsaturated trimetallic face with the $\mu_3\text{-}\eta^2$ (σ,π): η^2 (σ,π)-C_2 structure.[14] During their studies, a formal insertion of acetylide into a CH bond of dpmp has also been found through the isolation and characterization of $[Pt_3(\mu_3\text{-}\eta^2\text{-HCCH})(\mu\text{-dppm})_2\{\mu_2\text{-}\eta^3\text{-}(Ph_2P)_2CHCH{=}CH\}]^+$.[15]

Table 2. Selected Bond Distances (Å) and Angles (deg) for $[Pt_2Pd(\mu\text{-dpmp})(\mu\text{-}Ph_2PCH_2P(Ph)\text{-}CH_2P(Ph)_2C(CO_2Me)C(CO_2Me))(XylNC)_2](PF_6)_2$ (2)[a]

Bond Distances			
Pt(1)−Pt(2)	2.6792(4)	Pt(1)−P(3)	2.300(2)
Pt(1)−P(6)	2.275(2)	Pt(1)−C(2)	1.983(8)
Pt(2)···Pd(1)	3.3453(7)	Pt(2)−P(2)	2.292(2)
Pt(2)−P(5)	2.226(2)	Pt(2)−C(8)	2.138(7)
Pd(1)−P(1)	2.295(2)	Pd(1)−C(1)	1.999(8)
Pd(1)−C(7)	2.144(7)	Pd(1)−C(8)	2.067(7)
P(4)−C(5)	1.783(7)	P(4)−C(7)	1.794(7)
P(4)−C(411)	1.805(7)	P(4)−C(421)	1.800(7)
O(1)−C(31)	1.330(8)	O(1)−C(32)	1.440(9)
O(2)−C(31)	1.213(8)	O(3)−C(33)	1.359(8)
O(3)−C(34)	1.445(9)	O(4)−C(33)	1.212(8)
N(1)−C(1)	1.16(1)	N(1)−C(11)	1.41(1)
N(2)−C(2)	1.154(9)	N(2)−C(21)	1.399(9)
C(7)−C(8)	1.469(9)	C(7)−C(31)	1.481(9)
C(8)−C(33)	1.47(1)		

Bond Angles			
Pt(2)−Pt(1)−P(3)	87.97(5)	Pt(2)−Pt(1)−P(6)	92.61(5)
Pt(2)−Pt(1)−C(2)	160.3(2)	P(3)−Pt(1)−P(6)	168.85(7)
Pt(1)−Pt(2)−P(2)	88.75(5)	Pt(1)−Pt(2)−P(5)	84.88(5)
Pt(1)−Pt(2)−C(8)	155.3(2)	P(2)−Pt(2)−P(5)	165.78(7)
P(2)−Pt(2)−C(8)	97.5(2)	P(5)−Pt(2)−C(8)	93.5(2)
P(1)−Pd(1)−C(1)	100.5(2)	P(1)−Pd(1)−C(7)	143.4(2)
P(1)−Pd(1)−C(8)	105.0(2)	C(1)−Pd(1)−C(7)	113.6(3)
C(1)−Pd(1)−C(8)	154.2(3)	C(7)−Pd(1)−C(8)	40.8(3)
C(5)−P(4)−C(7)	109.9(3)	C(5)−P(4)−C(411)	105.0(3)
C(5)−P(4)−C(421)	104.0(3)	C(7)−P(4)−C(411)	114.9(3)
C(7)−P(4)−C(421)	112.6(3)	C(411)−P(4)−C(421)	109.6(3)
C(1)−N(1)−C(11)	173.4(9)	C(2)−N(2)−C(21)	174.6(7)
Pd(1)−C(1)−N(1)	172.6(8)	Pt(1)−C(2)−N(2)	168.8(7)
Pd(1)−C(7)−P(4)	116.8(3)	Pd(1)−C(7)−C(8)	66.8(4)
Pd(1)−C(7)−C(31)	106.6(4)	P(4)−C(7)−C(8)	127.4(5)
P(4)−C(7)−C(31)	106.8(5)	C(8)−C(7)−C(31)	122.8(6)
Pt(2)−C(8)−Pd(1)	105.4(3)	Pt(2)−C(8)−C(7)	131.9(5)
Pt(2)−C(8)−C(33)	104.7(4)	Pd(1)−C(8)−C(7)	72.4(4)
Pd(1)−C(8)−C(33)	125.5(5)	C(7)−C(8)−C(33)	115.4(6)

[a] Estimated standard deviations are given in parentheses.

(9) Pauling, L. *The Nature of the Chemical Bond*, 3rd ed.; Cornell University Press: New York, 1960; Chapter 7.

(10) Cotton, F. A.; Wilkinson, G. *Advanced Inorganic Chemistry*, 4th ed.; Wiley-VCH: New York, 1987; Chapter 27.

(11) (a) Ban, E.; Cheng, P.; Jack, T.; Nyburg, S. C.; Powell, J. *J. Chem. Soc., Chem. Commun.* **1973**, 368. (b) Jack, T. R.; May, C. J.; Powell, J. *J. Am. Chem. Soc.* **1977**, *99*, 4704. (c) Broadley, K.; Connelly, N. G.; Lane, G. A.; Geiger, W. G. *J. Chem. Soc., Dalton Trans.* **1986**, 373. (d) Connelly, N. G.; Geiger, W. E.; Orpen, A. G.; Orsini, J. J., Jr.; Richardson, K. E. *J. Chem. Soc., Dalton Trans.* **1991**, 2967. (e) Green, M.; Grove, D. M.; Howard, J. A. K.; Spencer, J. L.; Stone, F. G. A. *J. Chem. Soc., Chem. Commun.* **1976**, 759. (f) Boag, N. M.; Green, M.; Howard, J. A. K.; Spencer, J. L.; Stansfield, R. F. D.; Thomas, M. D. O.; Stone, F. G. A.; Woodward, P. *J. Chem. Soc., Dalton Trans.* **1980**, 2182. (g) Boag, N. M.; Green, M.; Howard, J. A. K.; Stone, F. G. A.; Wadepohl, H. *J. Chem. Soc., Dalton Trans.* **1981**, 862. (h) De Felice, V.; De Renzi, A.; Giordano, F.; Tesauro, D. *J. Chem. Soc., Dalton Trans.* **1993**, 1927.

(12) (a) Ciriano, M.; Howard, J. A. K.; Spencer, J. L.; Stone, F. G. A.; Wadepohl, H. *J. Chem. Soc., Dalton Trans.* **1979**, 1749. (b) Alcock, N. W.; Kemp, T. J.; Pringle, P. G.; Bergamini, P.; Traverso, O. *J. Chem. Soc., Dalton Trans.* **1987**, 1659. (c) Yam, V. W.-W.; Chan, L.-P.; Lai, T.-F. *Organometallics* **1993**, *12*, 2197. (d) Berenguer, J. R.; Fornies, J.; Lalinde, E.; Martinez, F. *J. Organomet. Chem.* **1994**, *470*, C15. (e) Berenguer, J. R.; Fornies, J.; Lalinde, E.; Martinez, F. *Organometallics* **1996**, *15*, 4537. (f) Ara, I.; Falvello, L. R.; Fornies, J.; Lalinde, E.; Martin, A.; Martinez, F.; Moreno, M. T. *Organometallics* **1997**, *16*, 5392. (g) Ara, I.; Falvello, L. R.; Fernandez, S.; Fornies, J.; Lalinde, A.; Martin, A.; Moreno, M. T. *Organometallics* **1997**, *16*, 5923.

(13) Tsutsumi, K.; Ogoshi, S.; Nishiguchi, S.; Kurosawa, H. *J. Am. Chem. Soc.* **1998**, *120*, 1938.

(14) (a) Douglas, G.; Manojlovic-Muir, L.; Muir, K. W.; Rashidi, M.; Anderson, C. M.; Puddephatt, R. J. *J. Am. Chem. Soc.* **1987**, *109*, 6527. (b) Manojlovic-Muir, L.; Muir, K. W.; Rashidi, M.; Schoettel, G.; Puddephatt, R. J. *Organometallics* **1991**, *10*, 1719. (c) Rashidi, M.; Schoettel, G.; Vittal, J. J.; Puddephatt, R. J. *Organometallics* **1992**, *11*, 2224.

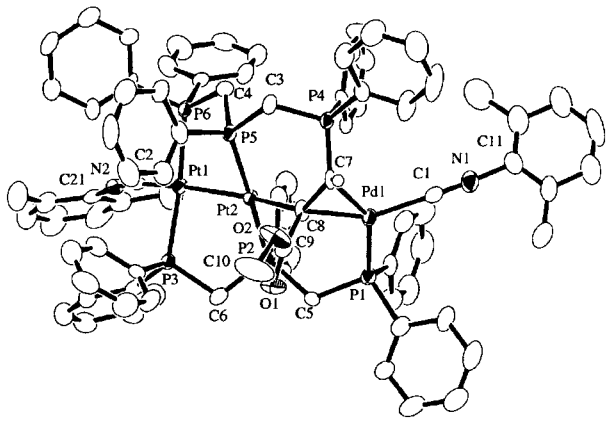

Figure 3. ORTEP plot of the complex cation of **4**, $[Pt_2Pd(\mu\text{-dpmp})(\mu\text{-}Ph_2PCH_2P(Ph)CH_2P(Ph)_2CHC(CO_2Me))(XylNC)_2]^{2+}$.

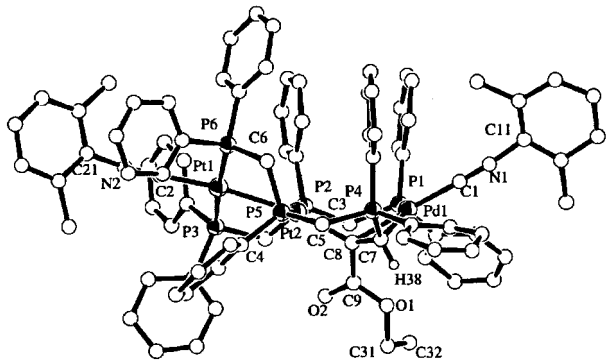

Figure 4. ORTEP plot of the complex cation of **5**, $[Pt_2Pd(\mu\text{-dpmp})(\mu\text{-}Ph_2PCH_2P(Ph)CH_2P(Ph)_2CHC(CO_2Et))(XylNC)_2]^{2+}$, viewed vertical to the Pt_2Pd plane. All atoms are drawn with ideal spheres.

Chart 1

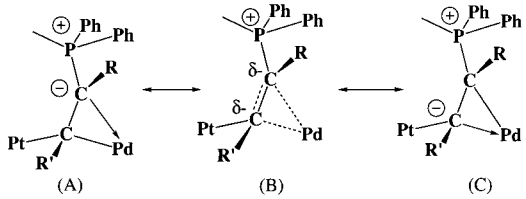

The geometry around P(4) is not unusual with four tetrahedrally arranged P−C bonds (1.783(7)−1.805(7) Å), strongly indicating a phosphorus ylide structure (zwitterionic structure) as described in Chart 1. The negative charge could be delocalized with resonance structures A, B, and C, which might lead to the stability of **2**−**6**. W. Lin et al. have reported the Pd-bound alkenyl phosphorus ylide complexes $[PdCl_2(Ph_2PCH_2P(Ph_2)HC{=}CR]$[16] as the first example of alkenyl phosphorus ylides of palladium derived from an unprecedented apparent insertion of alkynes into a palladium−phosphine bond.

The crystal structures of **4** and **5** are essentially similar to that of **2**. ORTEP diagrams for the complex cations of **4** and **5** are shown in Figures 3 and 4, respectively, and selected bond lengths and angles are listed in Tables 3 and 4. The $HC{\equiv}CCO_2R$ molecule was site-selectively inserted into the Pt−Pd bond and was further inserted into the Pd−P bond to form $\mu\text{-}\eta^1{:}\eta^2$-phosphorus ylide structures. The Pt−Pt bond distances are 2.6993(7) Å (**4**) and 2.696(1) Å (**5**), and the Pt···Pd

Table 3. Selected Bond Distances (Å) and Angles (deg) for $[Pt_2Pd(\mu\text{-dpmp})(\mu\text{-}Ph_2PCH_2P(Ph)\text{-}CH_2P(Ph)_2CHC(CO_2Me))(XylNC)_2](PF_6)_2$ (4)[a]

Bond Distances			
Pt(1)−Pt(2)	2.6993(7)	Pt(1)−P(3)	2.282(3)
Pt(1)−P(6)	2.284(3)	Pt(1)−C(2)	1.98(1)
Pt(2)···Pd(1)	3.6377(9)	Pt(2)−P(2)	2.298(3)
Pt(2)−P(5)	2.246(3)	Pt(2)−C(8)	2.119(9)
Pd(1)−P(1)	2.295(3)	Pd(1)−C(1)	2.02(1)
Pd(1)−C(7)	2.11(1)	Pd(1)−C(8)	2.11(1)
P(4)−C(3)	1.79(1)	P(4)−C(7)	1.77(1)
P(4)−C(411)	1.81(1)	P(4)−C(421)	1.81(1)
O(1)−C(9)	1.22(1)	O(2)−C(9)	1.34(1)
O(2)−C(10)	1.41(2)	N(1)−C(1)	1.12(1)
N(1)−C(11)	1.41(2)	N(2)−C(2)	1.15(1)
N(2)−C(21)	1.39(1)	C(7)−C(8)	1.42(1)
C(8)−C(9)	1.48(2)		

Bond Angles			
Pt(2)−Pt(1)−P(3)	85.38(7)	Pt(2)−Pt(1)−P(6)	92.24(7)
Pt(2)−Pt(1)−C(2)	167.3(3)	P(3)−Pt(1)−P(6)	168.2(1)
Pt(1)−Pt(2)−P(2)	84.46(7)	Pt(1)−Pt(2)−P(5)	87.17(7)
Pt(1)−Pt(2)−C(8)	174.7(3)	P(2)−Pt(2)−P(5)	170.2(1)
P(2)−Pt(2)−C(8)	95.3(3)	P(5)−Pt(2)−C(8)	93.5(3)
P(1)−Pd(1)−C(1)	102.8(3)	P(1)−Pd(1)−C(7)	145.1(3)
P(1)−Pd(1)−C(8)	105.9(3)	C(1)−Pd(1)−C(7)	112.1(4)
C(1)−Pd(1)−C(8)	151.1(4)	C(7)−Pd(1)−C(8)	39.3(4)
C(3)−P(4)−C(7)	107.1(5)	C(3)−P(4)−C(411)	107.1(5)
C(3)−P(4)−C(421)	107.0(5)	C(7)−P(4)−C(411)	109.0(5)
C(7)−P(4)−C(421)	118.0(5)	C(9)−O(2)−C(10)	116.5(9)
C(1)−N(1)−C(11)	177(1)	C(2)−N(2)−C(21)	170(1)
Pd(1)−C(1)−N(1)	178(1)	Pt(1)−C(2)−N(2)	171.9(9)
Pd(1)−C(7)−P(4)	117.6(6)	Pd(1)−C(7)−C(8)	70.3(6)
P(4)−C(7)−C(8)	122.1(8)	Pt(2)−C(8)−Pd(1)	118.7(5)
Pt(2)−C(8)−C(7)	128.9(8)	Pt(2)−C(8)−C(9)	103.7(7)
Pd(1)−C(8)−C(7)	70.4(6)	Pd(1)−C(8)−C(9)	116.3(7)
C(7)−C(8)−C(9)	116.6(9)		

[a] Estimated standard deviations are given in parentheses.

Table 4. Selected Bond Distances (Å) and Angles (deg) for $[Pt_2Pd(\mu\text{-dpmp})(\mu\text{-}Ph_2PCH_2P(Ph)\text{-}CH_2P(Ph)_2CHC(CO_2Et))(XylNC)_2](PF_6)_2$ (5)[a]

Bond Distances			
Pt(1)−Pt(2)	2.696(1)	Pt(1)−P(3)	2.282(5)
Pt(1)−P(6)	2.284(5)	Pt(1)−C(2)	1.93(2)
Pt(2)···Pd(1)	3.590(2)	Pt(2)−P(2)	2.274(5)
Pt(2)−P(5)	2.239(5)	Pt(2)−C(8)	2.04(2)
Pd(1)−P(1)	2.279(6)	Pd(1)−C(1)	1.98(2)
Pd(1)−C(7)	2.06(2)	Pd(1)−C(8)	2.16(2)
P(4)−C(5)	1.80(2)	P(4)−C(7)	1.79(2)
P(4)−C(411)	1.76(2)	P(4)−C(421)	1.81(2)
O(1)−C(9)	1.34(2)	O(1)−C(31)	1.48(3)
O(2)−C(9)	1.24(2)	N(1)−C(1)	1.16(2)
N(1)−C(11)	1.43(2)	N(2)−C(2)	1.18(2)
N(2)−C(21)	1.40(2)	C(7)−C(8)	1.40(2)
C(8)−C(9)	1.48(2)		

Bond Angles			
Pt(2)−Pt(1)−P(3)	87.5(1)	Pt(2)−Pt(1)−P(6)	88.7(1)
Pt(2)−Pt(1)−C(2)	171.7(4)	P(3)−Pt(1)−P(6)	174.0(2)
Pt(1)−Pt(2)−P(2)	87.7(1)	Pt(1)−Pt(2)−P(5)	84.4(1)
Pt(1)−Pt(2)−C(8)	168.9(5)	P(2)−Pt(2)−P(5)	171.7(2)
P(2)−Pt(2)−C(8)	93.2(5)	P(5)−Pt(2)−C(8)	95.0(5)
P(1)−Pd(1)−C(1)	105.8(6)	P(1)−Pd(1)−C(7)	139.2(6)
P(1)−Pd(1)−C(8)	101.1(5)	C(1)−Pd(1)−C(7)	114.7(8)
C(1)−Pd(1)−C(8)	153.1(7)	C(7)−Pd(1)−C(8)	38.8(7)
C(5)−P(4)−C(7)	107.2(9)	C(5)−P(4)−C(411)	105.6(8)
C(5)−P(4)−C(421)	109.0(9)	C(7)−P(4)−C(411)	117.8(9)
C(7)−P(4)−C(421)	109(1)	C(411)−P(4)−C(421)	107.9(9)
C(9)−O(1)−C(31)	115(2)	C(1)−N(1)−C(11)	175(2)
C(2)−N(2)−C(21)	168(2)	Pd(1)−C(1)−N(1)	176(2)
Pt(1)−C(2)−N(2)	168(1)	Pd(1)−C(7)−P(4)	118(1)
Pd(1)−C(7)−C(8)	74(1)	P(4)−C(7)−C(8)	125(1)
Pt(2)−C(8)−Pd(1)	117.4(8)	Pt(2)−C(8)−C(7)	128(1)
Pt(2)−C(8)−C(9)	114(1)	Pd(1)−C(8)−C(7)	67(1)
Pd(1)−C(8)−C(9)	106(1)	C(7)−C(8)−C(9)	113(2)

[a] Estimated standard deviations are given in parentheses.

(15) Jennings, M. C.; Manojlovic-Muir, L.; Puddephatt, R. J. *J. Am. Chem. Soc.* **1989**, *111*, 745.
(16) Allen, A., Jr.; Lin, W. *Organometallics* **1999**, *18*, 2922.

Scheme 3

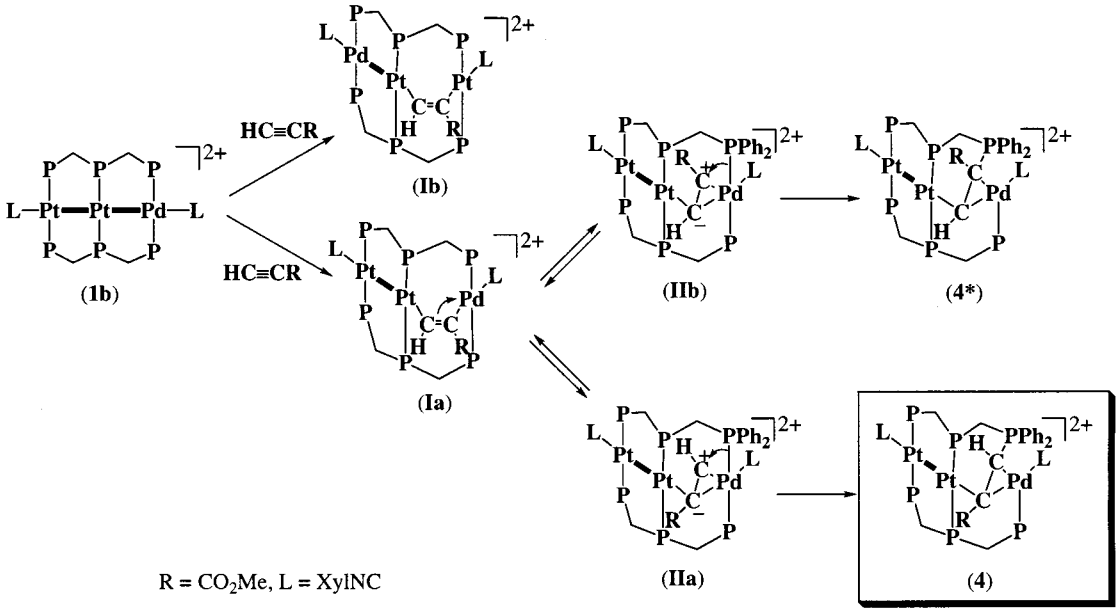

nonbonded distances are 3.6377(9) Å (**4**) and 3.590(2) Å (**5**). The Pt···Pd interatomic distances in **4** and **5** are significantly longer than is found in **2**, which can be ascribable to the lager Pt(2)−C(8)−Pd(1) angles (118.7(5)° (**4**) and 117.4(8)° (**5**)) than that of **2** (105.4(3)°). A remarkable difference from the structure **2** is shorter C−C bond lengths of the acetylene units (C(7)−C(8) = 1.42(1) Å (**4**) and 1.40(2) Å (**5**)), which fall between the values for C−C single and double bonds[9] and reflect a considerable contribution of the delocalized phosphorus ylide structure (B) as depicted in Chart 1. Furthermore, the site-selective insertion of alkynes is interestingly regiospecific. Only the terminal alkyne carbon (C(7)) of $HCCCO_2R$ reacted with phosphine to form the phosphorus ylide moieties, and the internal carbon (C(8)) with the electron-withdrawing substituent bridges the Pt(2) and Pd(1) atoms. This regiospecificity presumably results from the steric crowdedness of the phosphonium center over the palladium center, although the electronic factor cannot thoroughly be excluded. It should be noted that the regioselectivity observed in **4** and **5** is opposite of that found in the reaction of *linear*-$[Pt_3(\mu\text{-dpmp})_2(XylNC)_2]^{2+}$ (**1a**) with $HC{\equiv}CCO_2Me$ to form $[Pt_3(\mu\text{-dpmp})_2(\mu\text{-HC}{=}CCO_2Me)(XylNC)_2](PF_6)_2$ (**7c**) (Scheme 2).[2j] The terminal alkyne carbon is bound to the central Pt atom to avoid the steric repulsion on the central Pt vs on the terminal Pt atoms.

The novel structures of **2**, **4**, and **5** unambiguously determined by X-ray crystallography are retained in the solution state in the light of their ^1H and ^{31}P NMR spectra. It should be noted that the apparent double insertion of alkynes into metal−metal and metal−phosphine bonds elucidated in the present study was not observed with the analogous trimetallic compounds *linear*-$[M_3(\mu\text{-dpmp})_2(XylNC)_2](PF_6)_2$ (M = Pt (**1a**), Pd (**1c**)). As mentioned above, reaction of **1a** with activated alkynes led to the alkyne insertion only into one of the Pt−Pt bonds to generate the unsymmetrical Pt_3 clusters (**7a**−**c**) as shown in Scheme 2.[2j]

Formation Mechanism. Reaction of **1b** and $HC{\equiv}CCO_2Me$ was monitored by electronic absorption spectra. After an addition of $HC{\equiv}CCO_2Me$ to a dichloromethane solution of **1b**, the characteristic bands for **1b** (435, 393 nm) decreased and a new band at 348 nm increased with an isosbestic point at 375 nm. The reaction completed within 30 min, and finally, the spectral pattern came to be identical with that of **4**. These absorption spectral changes suggested that the apparent double insertion of the alkyne into Pt−Pd and Pd−P bonds occurred simultaneously and no stable intermediate species existed during the reaction at room temperature. We have speculated a plausible mechanism of the present reaction on the basis of the structures of **2**, **4**, **5** (Pt_2Pd), and **7c** (Pt_3) (Scheme 3). As an initial step, by analogy with the formation of **7c**, the alkyne molecule should be inserted into the Pt−Pd σ-bond to form a $\mu\text{-}\eta^1{:}\eta^1$-HC═CR ($2\sigma$) intermediate (**Ia**). The presence of the intermediate (**Ia**) could be confirmed by $^{31}P\{^1H\}$ NMR spectroscopy. The $^{31}P\{^1H\}$ NMR spectrum of the reaction mixture containing complex **1b** and $HC{\equiv}CCO_2Me$ at −20 °C showed predominant $AA'B_2C_2$ resonances at δ 15.1 (d × m, $^2J_{PP'}$ = 314 Hz), 7.85 (d × m, $^2J_{PP'}$ = 314 Hz), 1.51 (m, $^1J_{PtP}$ = 2855 Hz), and 0.69 (m, $^1J_{PtP}$ = 3133 Hz) in a ratio of 1:1:2:2. Whereas a perturbation around the Pd center occurred upon reaction, the spectral features are essentially similar to that of $[Pt_2(\mu\text{-Cl})PdCl(\mu\text{-dpmp})_2(XylNC)]^{2+}$ (**10**)[2j] and are consistent with the intermediate structure (**Ia**). When the temperature went up to 21 °C, the spectrum rapidly changed to one identical to that of the final product **4**. The higher nucleophilicity of Pd than Pt could be responsible for the site-selectivity of the insertion position between Pt−Pd and Pt−Pt σ-bonds. In the case of the Pt_3 system, compound **7c** including the $\mu\text{-}\eta^1{:}\eta^1$-HC═CR ($2\sigma$) unit was isolated and characterized by X-ray analysis.[2j] When insertion took place into the Pt−Pt bond, complex **Ib** should have been formed, but its formation was not confirmed by the NMR spectra of the reaction mixture. In complex **Ia**, an interaction of π electrons of the μ-HC═CR unit with the terminal Pd center led to zwitterionic polar activation of the C_2 unit as illustrated in **IIa**. Then, nucleophilic migration of the

Scheme 4

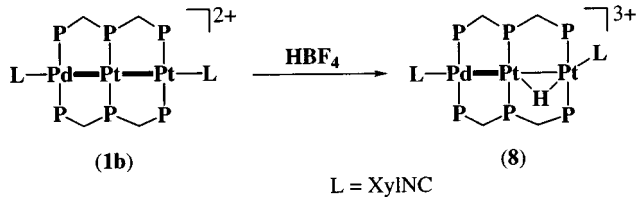

terminal P atom of the dpmp ligand from the Pd center to the CH terminal carbon afforded the isolated complex **4**. The π electron donation from the C_2 unit to Pd and the nucleophilic attack of the phosphine on the alkyne terminal carbon are estimated to proceed in a concerted mode. The bond formation between the phosphine and the internal alkyne carbon, leading to complex **4***, would not be favored owing to steric repulsion on the phosphorus center. The ^{1}H NMR spectrum of the reaction mixture did not indicate the presence of the isomer **4***.

Reaction of 1b with HBF_4 to Form $[Pt(\mu\text{-H})PtPd(\text{m-dpmp})_2(XylNC)_2](BF_4)_3$ (8). Treatment of **1b** with an excess of $HBF_4{\cdot}Me_2O$ gave the unsymmetrical trinuclear complex $[Pt_2Pd(\mu\text{-dpmp})_2(\mu\text{-H})(XylNC)_2](BF_4)_3{\cdot}CH_2Cl_2$ (**8**·CH_2Cl_2) in 62% yield (Scheme 4). Although the reaction proceeded quickly at room temperature, the isolated complex **8** is unstable in organic solvents and is likely to regenerate the linear trinuclear complex **1b** by a loss of a H atom. The analogous complex $[Pt_3(\mu\text{-dpmp})_2(\mu\text{-H})(XylNC)_2](BF_4)_3$ (**9**) has already been reported, but its structure was not characterized in detail.[2j] In the ^{1}H NMR spectrum, two singlets for the methyl groups of isocyanides were observed at δ 1.49 and 1.66, and the hydride peak was observed at δ −8.21 with two sets of satellite peaks due to coupling to two adjacent ^{195}Pt atoms ($^1J_{PtH}$ = 573 and 640 Hz). The ^{31}P-{^{1}H} NMR spectrum exhibited three multiplets at δ 11.8, −5.9, and −7.5 with a 1:1:1 ratio. The resonances at δ 11.8 and −7.5 are accompanied by ^{195}Pt satellite peaks with $^1J_{PtP}$ = 2210, 2618 Hz and that at δ −5.9 appeared without ^{195}Pt satellite.

The structure of **8** was determined by X-ray crystallography, as illustrated in Figure 5. Selected bond lengths and angles are listed in Table 5. The complex cation is composed of a Pt−Pt−Pd trimetallic core which is bridged by two dpmp ligands and is terminally capped by two isocyanide molecules. The Pt_2Pd atoms are arranged in a linear fashion with the Pt(1)−Pt(2)−Pd(1) angle of 174.41(7)° (Figure 5b). The Pt(2)−Pd(1) distance of 2.634(3) Å demonstrates the presence of a Pt−Pd bond; however, the Pt(1)−Pt(2) distance of 2.867(2) Å is significantly longer than those observed in **1a** (av 2.724 Å) and **1b** (av 2.690 Å) and is not a value for a normal Pt−Pt single bond. The Pt−Pt distance in **8** is slightly shorter than is found in $[Pt_2Me_2(\mu\text{-H})(\mu\text{-dppm})_2](PF_6)_2$ (2.932(1) Å)[17] and is indicative of a weak metal−metal bonding interaction. The hydrogen atom (H(1)) was found by difference Fourier synthesis to sit between the Pt(1) and Pt(2) atoms. The hydrogen bridge is asymmetrical with Pt(1)−H(1) = 1.94 Å, Pt(2)−H(1) = 2.14 Å, and Pt(1)−H(1)−Pt(2) = 88.9°. The terminal isocyanide attached to Pt(1) is deformed from collinear

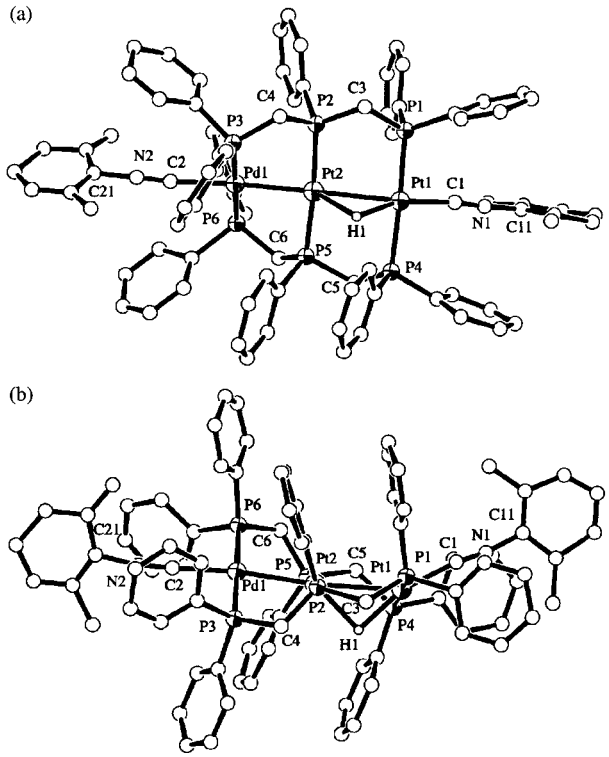

Figure 5. (a) ORTEP view of the complex cation of **8**, $[Pt_2Pd(\mu\text{-dpmp})_2(\mu\text{-H})(XylNC)_2]^{3+}$, and (b) a diagram viewed vertical to the Pt_2Pd plane. All atoms are drawn with ideal spheres.

Table 5. Selected Bond Distances (Å) and Angles (deg) for $[Pt_2Pd(\mu\text{-dpmp})_2(\mu\text{-H})(XylNC)_2](BF_4)_3$ (8)[a]

Bond Distances			
Pt(1)−Pt(2)	2.867(2)	Pt(1)−P(1)	2.323(7)
Pt(1)−P(4)	2.350(6)	Pt(1)−C(1)	2.03(3)
Pt(2)−Pd(1)	2.634(3)	Pt(2)−P(2)	2.299(7)
Pt(2)−P(5)	2.280(7)	Pd(1)−P(3)	2.342(7)
Pd(1)−P(6)	2.294(7)	Pd(1)−C(2)	2.13(4)
N(1)−C(1)	1.06(3)	N(1)−C(11)	1.40(4)
N(2)−C(2)	1.12(5)	N(2)−C(21)	1.46(5)

Bond Angles			
Pt(2)−Pt(1)−P(1)	87.4(2)	Pt(2)−Pt(1)−P(4)	89.8(2)
Pt(2)−Pt(1)−C(1)	148.8(9)	P(1)−Pt(1)−P(4)	175.9(3)
Pt(1)−Pt(2)−Pd(1)	174.41(7)	Pt(1)−Pt(2)−P(2)	93.8(2)
Pt(1)−Pt(2)−P(5)	91.2(2)	Pd(1)−Pt(2)−P(2)	88.6(2)
Pd(1)−Pt(2)−P(5)	86.2(2)	P(2)−Pt(2)−P(5)	174.2(3)
Pt(2)−Pd(1)−P(3)	88.3(2)	Pt(2)−Pd(1)−P(6)	92.6(2)
Pt(2)−Pd(1)−C(2)	174.0(9)	P(3)−Pd(1)−P(6)	179.1(3)
C(1)−N(1)−C(11)	170(4)	C(2)−N(2)−C(21)	171(4)
Pt(1)−C(1)−N(1)	170(3)	Pd(1)−C(2)−N(2)	175(3)

[a] Estimated standard deviations are given in parentheses.

position with the Pt_2Pd core (Pt(2)−Pt(1)−C(1) = 148.8(9)°) and is arranged in a *trans* position to the H(1) atom (C(1)−Pt(1)−H(1) = 159.0°). The crystal structure revealed that oxidative addition of H^+ to the Pt−Pt bond of **1b** led to the hydride-bridged Pt_2Pd cluster **8**, with a slight tilting of the terminal isocyanide and a slight elongation of the Pt−Pt bond (Chart 2). The core structure of **8** is quite different from that of the unsymmetrical trimetallic A-frame cluster, as observed in $[Pt_2PdCl(\mu\text{-Cl})(\mu\text{-dpmp})_2(XylNC)_2](PF_6)_2$ (**10**),[2j] where the chloride bridge completely breaks the Pt−Pd bond (3.103(3) Å) (Chart 2).

The ^{1}H NMR spectrum of the reaction mixture of **1b** with HBF_4 showed a major hydride peak at −8.21 ppm for the Pt(μ-H)PtPd cluster **8** and a minor peak at −8.45

(17) Brown, M. P.; Cooper, S. J.; Frew, A. A.; Manojlovic-Muir, L.; Muir, K. W.; Puddephatt, R. J.; Thomson, M. A. *J. Chem. Soc., Dalton Trans.* **1982**, 299.

Chart 2

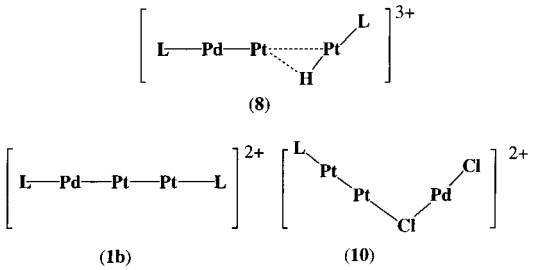

L = XylNC and dpmp ligands are omitted.

ppm with an integration ratio of 9:1. The minor peak is assumed to correspond with the PtPt(μ-H)Pd cluster, although its isolation was not successful. Consequently, the oxidative insertion of H^+ occurred site-selectively into the Pt−Pt bond, which could be due to higher stability of the Pt−H bond than that of the Pd−H bond[10] and is interestingly contrasted with the opposite selectivity observed with activated alkynes.

Conclusion

In this study, an unprecedented double insertion of electron-deficient alkynes was found through reactions of the Pt_2Pd heterotrimetallic complex **1b** with RC≡CR′ leading to a series of unsymmetrical Pt_2Pd A-frame complexes with a μ-η^1:η^2-phosphorus C_2 ylide moiety (**2**−**6**). The insertion took place site-selectively into the Pt−Pd bond vs the Pt−Pt bond, and P−C bond formation occurred on the terminal alkyne carbon regioselectively. In contrast, reaction of **1b** with HBF_4 afforded [Pt_2Pd(μ-dpmp)$_2$(μ-H)(XylNC)$_2$](BF_4)$_3$ (**8**), in which the H atom was inserted into the Pt−Pt bond rather than the Pt−Pd bond with a slight structural change of the cluster core. These results demonstrated that the heterometal (Pd) was able to alter the reactivity of the linear trimetallic clusters and interestingly regulated its specificity, and could provide useful information in developing multifunctional heterometallic catalysts.

Acknowledgment. This work was partially supported by a Grant-in-Aid for Scientific Research from the Ministry of Education of Japan.

Supporting Information Available: Tabulations of crystallographic data, positional and thermal parameters, and bond lengths and angles of non-hydrogen atoms for **2**, **4**, **5**, and **8**. This material is available free of charge via the Internet at http://pubs.acs.org.

OM000747Y